

# 林业复杂地形动力底盘性能主要影响因素分析

曲振兴<sup>1</sup>, 向文博<sup>1,2</sup>, 胡景阳<sup>1</sup>, 王凡<sup>1,2</sup>, 周建波<sup>3\*</sup>

(1. 国家林业和草原局哈尔滨林业机械研究所, 哈尔滨 150086;

2. 中国林业科学研究院研究生部, 北京 100000)

**摘要:** 对影响林业复杂地形动力底盘性能的几种因素进行介绍, 从林地坡度与地面环境、动力底盘的稳定性、通过性及爬坡度进行分析, 得出三个主要影响因素, 分别是: 动力底盘重心位置的布置、前后轮轴心位置的布置与轮胎的选取 (包括半径及花纹等), 为动力底盘的设计提供一定参考。

**关键词:** 林业复杂地形; 动力底盘; 性能影响因素

## Analysis on main influencing factors of dynamic chassis performance in forestry complex terrain, China

**Abstract:** This paper introduces several factors that affect the performance of the power chassis in complex forestry terrain. From the analysis of the woodland slope and ground environment, the stability of the power chassis, the passability and the grade of climbing, three main influencing factors are obtained, namely: the center of gravity of the power chassis. The arrangement of the position, the arrangement of the axle center of the front and rear wheels and the selection of the tires (including the radius and pattern, etc.) provide a certain reference for the design of the power chassis.

**Key words:** forestry complex terrain; power chassis; performance impact factors

动力底盘在我国林业机械化发展进程中有至关重要的影响地位, 尤其是目前动力底盘缺失导致的林业机械设备上山难、行走难现状<sup>[1]</sup>。林地环境复杂, 地面平整度以及抚育管理程度与田地相比有极大差距, 林地自身坡度条件、地面沟壑障碍都对动力底盘的稳定性以及通过性提出了很高的要求。在进行动力底盘设计时, 要充分考虑到林地自身条件对其结构、性能的影响, 在满足安全的前提下, 提高动力底盘的性能。本文主要从林地坡度、动力底盘的稳定性、通过性及爬坡度四个角度研究对哪些因素动力底盘的性能产生影响。

### 1 林地坡度与地面环境

表示坡度最为常用的方法是采用两点间的高程差与其水平距离的百分比。目前我国对坡度大小的分级, 一般分为六级: 平坡: 0-5 度; 缓坡: 6-15 度; 斜坡: 16-25 度; 陡坡: 26-35 度; 急坡: 36-45 度; 险坡: 大于 46 度<sup>[2]</sup>。25 度坡度以上的土地为《水土保持法》规定的开荒限制坡度, 即不准开荒种植农作物。因此, 在设计林业动力底盘时, 可以 25 度坡度以下的林地作为研究对象, 讨论各因素对林业动力底盘的影响。

林地复杂地面环境对于动力底盘的各项性能提出较高的要求。在对人工开发出的经济林地进行需求设计时, 要充分考虑种植密度 (行距、株距) 对动力底盘及整体尺寸的要求, 同时转向方式简单, 转弯半径

第一作者简介: 曲振兴 (1982—), 女, 高级工程师, 硕士, 主要从事营林机械技术装备应用研究, E-mail: qzx\_2@163.com。

\*通讯作者: 周建波 (1983—), 男, 研究员, 博士, 主要从事竹材加工技术机械的研究, E-mail: zhoujianbol@126.com。

要尽可能小，在林地间工作时要灵活轻便<sup>[3]</sup>。此外在进行轮胎选择时要考虑土壤特性，如林地多雨，土壤较为潮湿，整体硬度较低，对于轮胎选择有一定要求<sup>[3]</sup>。若所选轮胎花纹太浅，在发生抓地力与附着力不足的情况时，易发生打滑或越障失败，若轮胎花纹太深，则需要考虑轮胎转动时是否能甩掉花纹间携带的泥土。

## 2 稳定性

### 2.1 纵向稳定性

当运动底盘以低速匀速上坡时，忽略空气阻力，视轮胎为刚性体，进行力学分析，如图 9，建立力学平衡方程：

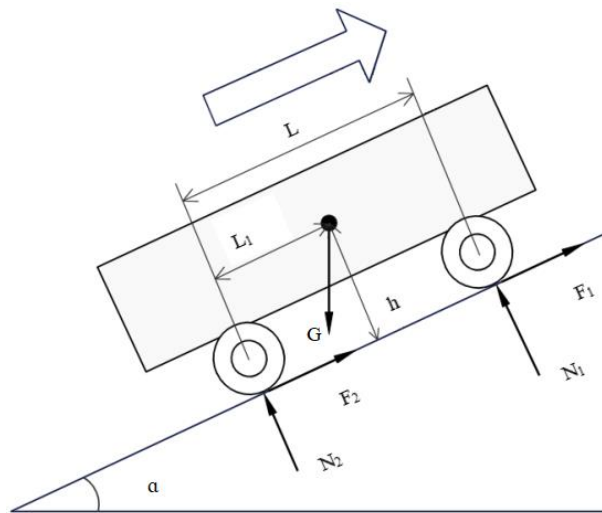


图 9 低速匀速上坡受力图

Fig. 1 Low speed and uniform uphill force diagram

$$\begin{cases} F_1 + F_2 = G \sin \alpha \\ N_1 + N_2 = G \cos \alpha \\ Gh \sin \alpha + N_1 L = GL_1 \cos \alpha \end{cases}$$

式中：

$F_1$ ——土壤对前轮切向作用力

$F_2$ ——土壤对后轮切向作用力

$G$ ——底盘重力

$\alpha$ ——上坡极限翻倾角

$N_1$ ——土壤对前轮的法向作用力

$N_2$ ——土壤对后轮的法向作用力

$h$ ——重心到地面的垂直高度

$L$ ——前后轮轴心水平距离

$L_1$ ——重心到后轮轴心水平距离

当前轮刚好不受土壤反作用力时，达到上坡倾翻极限状态，此时  $F_1 = 0$ ，可得上坡极限倾翻角

$$\alpha_{lim} = \arctan \frac{L_1}{h}$$

当底盘的后轮刚好不受土壤的反作用力时，即为下坡极限倾翻临界状态，则后轮的切向作用力  $F_2 = 0$ ，

$$\begin{cases} F_1 + F_2 = G \sin \alpha' \\ N_1 + N_2 = G \cos \alpha' \\ Gh \sin \alpha' + N_2 L = G(L - L_1) \cos \alpha' \end{cases}$$

可得下坡极限倾翻角为

$$\alpha'_{lim} = \arctan \frac{L - L_1}{h}$$

由式可知，底盘的倾翻极限角与重心位置有关，重心越低，底盘的倾翻极限角越大，同时重心越接近较低轮着地点，底盘的倾翻极限角越大。

因此，结合上下坡的使用需求，在设计时将重心布置在底盘中段尽可能低的位置，能增大底盘的倾翻极限角，增强稳定性。

### 2.2 横向稳定性

底盘在倾斜路面上静止或行驶过程中，在横向力的作用下，可能产生沿横向力方向的侧向滑移，如图 10。不产生横向滑移的最大坡度角称为横向滑移角  $\varphi$ 。满足稳定条件是横向力小于等于轮胎与路面之间的横向附着力<sup>[5]</sup>。

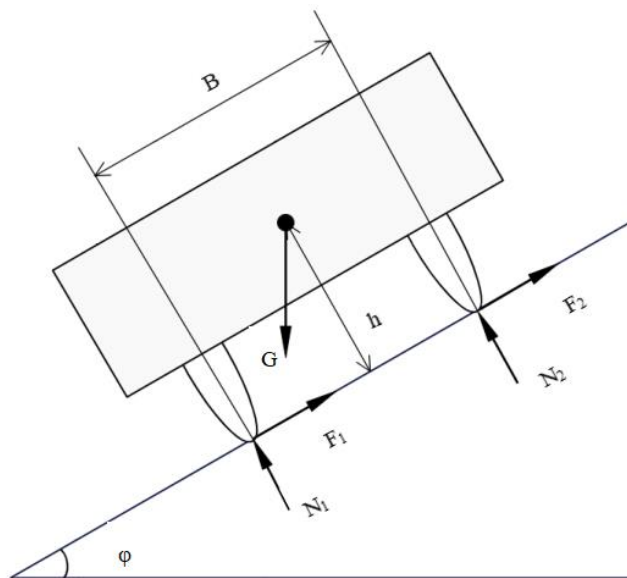


图 10 横向受力图

Fig. 2 Lateral force diagram

$$G \sin \varphi = G \cos \varphi \cdot \Phi$$

$$\varphi = \text{tg}^{-1} \Phi$$

式中：

$\Phi$ ——横向附着系数，是指支撑面提供的最大切向力与支撑面法向反作用力之比。

由此可知，横向滑移角  $\varphi$  仅取决于横向附着系数  $\Phi$ 。附着系数受到道路状况、轮胎花纹样式等影响较大，在选择轮胎时注意选择花纹样式较深，并且注意路况，避免发生横向滑移。

### 3 通过性

影响车辆通过性的因素主要有：最小离地间隙、接近角、离去角以及纵向通过角等。

车辆在通过起伏不平的路面时，地面的凸起障碍会发生拖住底盘底部的情况，发生“顶起失效”，使底盘无法通过<sup>[6]</sup>，这种情况是由于在底盘设计时，没有充分考虑到最小离地间隙和纵向通过角导致的。

当动力底盘在崎岖路面通过时，首先要考虑到地面的垂直高度差与底盘底部到地面的间隙之间的关系，如图 11。若设置的最小离地间隙过小，可能导致地面顶起底盘无法前进的问题。最小离地间隙与底盘自身结构布局以及轮胎的选取有关。最小离地间隙的测量点应选取底盘最低点，因此底盘结构应布置的尽量平整，避免出现尖锐凸起，影响最小离地间隙。另一个影响最小离地间隙的因素是轮胎的选取。增大轮胎的直径可以提高底盘的离地间隙，降低轮胎的接地比压，增加与地面接触面积以减少土壤阻力和滑转，但会升高底盘整体重心位置，同时要采用大传动比的传动系传输动力，因此在选取轮胎时，要充分考虑到最小离地间隙与重心位置间的影响关系。

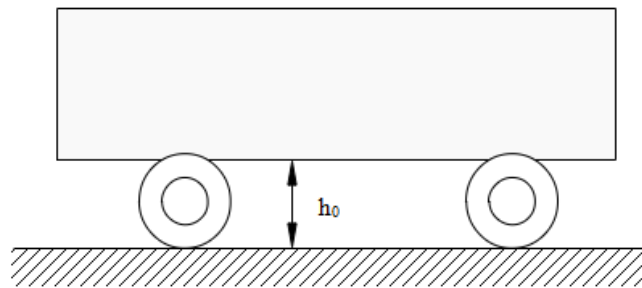


图 11 最小离地间隙示意图

Fig. 3 Schematic diagram of minimum ground clearance

纵向通过角是车辆在满载、静止时，分别通过前、后轮胎外缘作垂直于车辆纵向对称平面的切平面，当两平面交于车体下部最低部位时所夹的最小锐角  $\beta$ <sup>[7]</sup>，如图 12。纵向通过角与最小离地间隙以及前后轮轴心水平距离有关。最小离地间隙越大，纵向通过角越大，此时底盘重心升高，极限倾翻角减小，稳定性降低。前后轮轴心水平距离变大，纵向通过角减小，此时底盘极限倾翻角变大，稳定性提升。

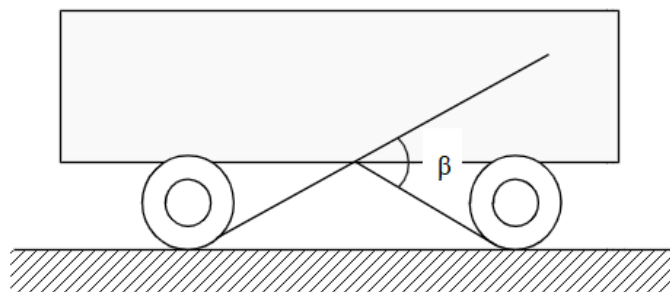


图 12 纵向通过角示意图

Fig. 4 Schematic diagram of longitudinal passage angle

接近角与离去角是车辆前后边缘与车辆前后轮所引切线与地面的夹角，如图 13。在行驶过程中，若车辆前后端伸出过长，会导致  $\gamma_1$  或  $\gamma_2$  减小，车辆前后缘触及地面，发生“触头失效”或“拖尾失效”，也易

发生不能通过的问题<sup>[8]</sup>。

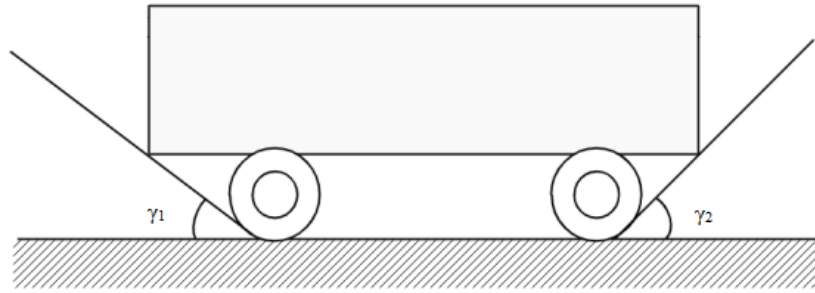


图 13 接近角与离去角示意图

Fig. 5 Schematic diagram of approach angle and departure angle

#### 4 爬坡度

动力底盘在进行林间作业和运输过程中，通常属于满载、低速的运动状态，车速变化不大，几乎不产生加速超车情况，因此用爬坡度评估动力底盘在坡地工作的爬坡能力，设驱动底盘在坡度角为  $\alpha$  的坡道上用变速箱最低档位保持等速行驶，此时的运动平衡方程式为：

$$F_q = F_w + F_f + G \sin \alpha$$

式中：

$F_q$ ——底盘驱动力

$F_w$ ——空气阻力： $F_w = \frac{C_D A v^2}{21.15}$ ， $C_D$ ——空气阻力系数， $A$ ——迎风面积， $v$ ——行驶速度

$F_f$ ——滚动阻力： $F_f = fG \cos \alpha$ ， $f$ ——滚动阻力系数

由发动机输出的有效扭矩和传动系数参数，可计算驱动底盘在最低档位时动力底盘所产生的最大驱动力为：

$$F_q = \frac{M_e i_g i_0 \eta_T}{r}$$

式中：

$M_e$ ——发动机扭矩

$i_g$ ——变速器各档位比

$i_0$ ——主减速器速比

$\eta_T$ ——传动系统总效率

$r$ ——车轮滚动半径

对于林用动力底盘设计来说，对行驶速度的要求并不高，在根据林地环境确定整体车型后，即可确定  $F_w$  空气阻力；根据地面情况确定滚动阻力系数后，可确定  $F_f$  滚动阻力，由此得出所需的底盘驱动力。底盘驱动力与发动机扭矩成正比，与车轮滚动半径成反比。为了增大底盘驱动力选取大扭矩发动机会提高制造成本，减小车轮滚动半径则会影响运动底盘的通过性能。

#### 5 综合分析

本文介绍了几种影响林地动力底盘性能的因素：林地坡度与地面环境、动力底盘稳定性、通过性与爬坡度。林地坡度与地面环境作为背景因素，是进行动力底盘设计制造的前提条件。在设计之前，要着重考察动力底盘的工作环境、土壤物理性质、林地种植密度（行距、株距）等因素，对动力底盘及整机外形尺寸结构有一定的指导意义，确立尺寸要素。

动力底盘的稳定性、通过性与爬坡度作为动力底盘工作性能的代表，通过分析得知三性能互相影响。三个主要影响因素：动力底盘重心位置的布置、前后轮轴心位置的布置与轮胎的选取（包括半径及花纹等），在设计过程中要充分考虑关联关系，在满足林地背景因素条件的基础上降低重心提升稳定性、提升运动底盘的通过性能。

## 参考文献

- [1] 张昊,樊桂菊,王永振.果园机械底盘发展现状与趋势分析[J].中国农机化学报,2017,38(10):121-125.
- [2] 陈绍玲.山地丘陵坡度与林业施策问题的探讨[J].华东森林经理,2009,23(01):17-21.
- [3] 汤晶宇,寇欣,徐克生,吴昊,曲振兴,王德柱,樊涛.丘陵地区经济林内动力底盘研究现状分析[J].林业机械与木工设备,2019,47(12):4-8.
- [4] 洪桂香.汽车轮胎花纹与轮胎的性能[J].时代农机,2015,42(05):168-169.
- [5] 唐兆家,王凤花,喻黎明.轮式拖拉机行驶稳定性分析[J].农业装备与车辆工程,2018,56(05):15-19.
- [6] 邱垂翔,胡彭俊,张启亮.乘用车最小离地间隙设定方法的研究[J].汽车零部件,2021(11):49-52.
- [7] 刘庆上,姚兰杰.汽车纵向通过角理论及其作图求法浅析[J].汽车科技,2014(04):12-16.
- [8] 刘爽,唐兴贵,应宇汀,康燕妮.汽车接近角及离去角定义及检测方法概述[J].时代汽车,2018(03):30-32.
- [9] 王锋.丘陵山地果园动力底盘的坡地通过性研究[D].西南大学,2020.

## Influence of Different Precipitation Periods on *Dendrolimus superans* Occurrence: A biostatistical Analysis

Zhiru Li<sup>4,2</sup>, Zhenkun Miao<sup>1,2</sup>, Xiaofeng Wu<sup>1,2,\*</sup>, Beihang Zhang<sup>1,2</sup>, Quangang Li<sup>1,2</sup>, Lizhi Han<sup>1,2</sup>, Jun Wang<sup>3</sup>

(1. Harbin Research Institute of Forestry Machinery, the State Forestry and Grassland Administration, Harbin, 150086, P.R. China

2. Research Institute of Forestry New Technology, Beijing, 100091, P.R. China

3. Forest Pest Control and Quarantine Station of Yichun City, Yichun 153000, P.R. China)

**Abstract:** Precipitation is one of the most important abiotic factors that affect *Dendrolimus superans* occurrence. In this study, a grey slope-correlation model was used, and a simplified grey slope-correlation model was constructed to uncover the most crucial periods of precipitation that pest occurrence. Results revealed that the two models are very similar; however, the simplified grey slope-correlation model required less calculative steps and was easier to operate. The calculation results revealed that the most crucial period occurred during the first 10 days of July ( $\gamma_{13} = 0.67, \gamma'_{13} = 0.69$ ). The other precipitation periods associated with pest occurrence included the first 10 days of August ( $\gamma_{16} = 0.62, \gamma'_{16} = 0.61$ ), the third 10 days of May ( $\gamma_{09} = 0.59, \gamma'_{09} = 0.62$ ), the second 10 days of May ( $\gamma_{08} = 0.58, \gamma'_{08} = 0.60$ ), and the third 10 days of August ( $\gamma_{18} = 0.58, \gamma'_{18} = 0.60$ ). The less associated precipitation periods included the first 10 days of March ( $\gamma_{01} = 0.54, \gamma'_{01} = 0.47$ ), the second 10 days of March ( $\gamma_{02} = 0.50, \gamma'_{02} = 0.49$ ), the third 10 days of April ( $\gamma_{06} = 0.47, \gamma'_{06} = 0.48$ ), the second 10 days of June ( $\gamma_{11} = 0.51, \gamma'_{11} = 0.48$ ), and the third 10 days of June ( $\gamma_{12} = 0.51, \gamma'_{12} = 0.51$ ). Precipitation in May ( $\gamma_{07} + \gamma_{08} + \gamma_{09} = 1.74, \gamma'_{07} + \gamma'_{08} + \gamma'_{09} = 1.79$ ) and July ( $\gamma_{13} + \gamma_{14} + \gamma_{15} = 1.74, \gamma'_{13} + \gamma'_{14} + \gamma'_{15} = 1.79$ ) was mostly associated with *D. superans* occurrence. The findings of this study provided a simple operative model for determining the most crucial precipitation periods of pest occurrence, and these analytical methods can serve as a theoretical reference for pest forecasting and early warning, which is contribute to ecological protection.

**Key words:** *Dendrolimus superans*; Grey slope correlation; Occurrence; Precipitation; Simplified model.

The occurrence of forest pests, which are known as “the no-smoke forest fire,” are likely to cause tree die-out, ecological destruction, and subsequently reduce forest carbon sequestration (Xu *et al.* 2015). *Dendrolimus superans* (Butler) is the main leaf-eating insect found in the northeastern forests of China, which turns tree branches bleak when its larvae gnaw the leaves (Dang *et al.* 2018). *D. superans* can also be found in other regions under similar latitude and climatic conditions (Kang 2005; Tomin *et al.* 2011; Myong *et al.* 2012). The pests outbreaks vary greatly depending on the environment and climatic conditions, and the degree of damage, spreading direction, and duration of different stages can be forecast by studying the growth ratio of larvae (Natalia *et al.* 2009).

The occurrence of forest pests is a result of many factors, including biological characteristics, natural enemies, meteorological conditions, site conditions, and stand structure (Chen *et al.* 2017). The relationship between meteorological factors and the occurrence of forest pests is a system consisting of many mathematical inputs. These inputs have an interactive effect with one another, including evaporation capacity, precipitation, average temperature, and accumulated temperature (Tang and Niu. 2010). However, it is difficult to formulate the relationship between a designated meteorological factor and the occurrence of forest pests (Feng *et al.* 2013). Most of the existing research has obtained an approximate relationship between these two factors through data integration, analysis, and exploration, and most of these results were non-linear (Zhang *et al.* 2012; Abdul *et al.* 2014).

Previous studies on the relationship between the occurrence of forest pests and meteorological factors in Northern China have revealed that temperature and precipitation during the spring and summer were the most critical factors influencing pest population (Tang and Niu. 2010; Chen *et al.* 2011). This influence was greater at the larval stage, while the annual accumulated temperature (The sum, counted in degrees, by which the actual air temperature rises above or falls below a datum level over a year), annual precipitation, and dryness had the greatest Pearson correlation coefficients with pest area (Yang *et al.* 2014; Nie *et al.* 2017). A similar study concluded that extreme heat or cold had little effect on annual catches of *Ips typographus*, while growth rate had a linear relationship with temperatures between 15 and 25°C (Bakke 1992; Wermelinger and Seifert. 1998). In a separate study, *Diprionhercyniae* outbreak was induced by the hot and dry climate and severe low moisture (Marchisio *et al.* 1994). Moreover, a stepwise regression analysis revealed that the daily average temperature during the winter and precipitation during the breeding season was a key factor influencing population fluctuations of *D. superans*, while the larval stage and breeding season were the most critical periods (Yu *et al.* 2016).

More and more novel algorithms are being used for pest control and forecasting by utilizing big data and information on climate globalization (Kumar 2015). The artificial neural network, multilayer feedforward neural network (MLFN), generalized regression neural network (GRNN), support vector machine (SVM), and other algorithms have been used to forecast the occurrence of pest, and these machine learning measures have been more accurate

基金项目: the Central Non-Profit Research Institution of the Chinese Academy of Forestry (No. CAFYBB2018QA011).

\*为通讯作者

than multiple linear regression predictions (Chon *et al.* 2000; Zhang *et al.* 2017; Rathee and Kashyap. 2018 ). However, like other system analysis methods in machine learning measures, regression analyses require mass data and expect much of the data to take on a typical probability distribution (e.g., linear, exponential, logarithmic, and so on). Multiplication, division, and power operations are often involved in the computational process, but small errors can result in serious errors, which lead to discrepancies between the quantitative results and qualitative analysis. This may also lead to a relationship between systems that cannot be objectively expressed (Cao 2007; Liu and Xie. 2013). Additionally, due to the complexity of computational models, they are not widely used by forest workers or researchers. Therefore, when the grey correlation analysis is used to study the relationship between meteorological variation and pest occurrence, the vector set was easy to divided and call for no more others variables, the model needs to possess less calculative complexity and be easy to operate.

In this study, the selected meteorological index was easy to calculate and the system did not affect the simplicity or functioning of the model. Thus, this analytical method and the findings of this study can serve as a theoretical reference for pest forecasting and early warning. For example, this analytical method and the findings can be widely use for forest worker, when precipitation during the first 10 days of July ( the Breeding season of *D. superans*) was less than others year, we should be careful the *D. superans* outbreak next year.

## 1 Materials and Methods

### 1.1 Location and status of the studied habitats

This study was conducted in the southeast of Xiaoxinganling Mountains located in Tieli of Yichun City, Heilongjiang Province, China. Regional vegetation mainly includes *Pinus koraiensis*, *Larix gmelinii*, and *Picea jezoensis*. As for the climate, the winters are long and the summer is short. The maximum air temperature may exceed 35°C, while the minimum air temperature can drop below -41°C. Meteorological data were collected from the Tieli weather station (128°01'E and 46°59'N). The altitude of the observation site was 210.5 m, and the altitude of the sensor of the barometer was 213.4 m. The height of the wind speed sensor to the platform was 9.36 m, while the height of the observation platform to the ground was 11.76 m.

### 1.2 Statistics and data compilation

A grey correlation analysis was used to study the relationship between meteorological variation and pest occurrence. The selection of characteristic data is key for the foundation of this analysis. *D. superans* occurrence from 1997 to 2017 was used as the main time period response sequence:  $X_0$  and  $X_0 = x_0(k)$  ( $k = 1, 2, \dots, n$ ), then  $X_i = x_i(k)$  ( $i = 1, 2, \dots, m, k = 1, 2, \dots, n$ ) ( $n = 21$ ), where  $x_i$  was the  $i$ th influencing factor of the system and  $X_i$  ( $i = 1, 2, \dots, n$ ) was the characteristic time response data sequence. The analysis in same sample plot did not consider the soil composition, stand structure, or human disturbance, which made *D. superans* occurrence of Tieli the main data sequence, while the temperature, precipitation, average wind speed, and other time node meteorological data were used as the characteristic data sequences. The grey correlation degree was acquired by the grey correlation analysis, and the degree revealed that precipitation during the spring and summer had the greatest effect on *D. superans*' occurrence (Li *et al.* 2019).

Therefore, the influence of different precipitation parameters on *D. superans* occurrence was investigated further. In this analysis, *D. superans* occurrence from 1997 to 2017 was the main time response sequence:  $X_0$ , and  $X_i = x_i(k)$  ( $i = 1, 2, \dots, m, k = 1, 2, \dots, n$ ) ( $m = 18, n = 21$ ), where  $X_i$  was the different precipitation periods from March to August. Each month was divided into 3 parts,  $x_1, x_2$ , and  $x_3$ , which represent the first, second, and third 10 days of March, while  $x_4, x_5$ , and  $x_6$  represent the first, second, and third 10 days of April; this pattern spanned through August until  $x_{18}$  (Table 1). Then, the correlative relationship between precipitation and *D. superans* occurrence was



investigated.

**Tab.1 The characteristic sequence data table**

	1997	1998	1999	2000	2001	2002	2003	2004	2005	2006	2007	2008	2009	2010	2011	2012	2013	2014	2015	2016	2017
$X_0/(\times 10^9 \text{hm}^2)$	4.07	7.73	5.05	3.25	3.07	2.75	4.13	2.87	1.67	1.24	1.31	0.95	0.9	0.98	0.8	0.75	0.35	0.35	0.28	0.34	0.48
$X_1/(0.1\text{mm})$	5	0	6	25	73	0	28	0	32	99	21	147	62	0	18	41	7	37	122	40	63
$X_2/(0.1\text{mm})$	22	204	51	68	36	0	1	67	51	30	4	63	44	193	75	3	0	30	127	10	38
$X_3/(0.1\text{mm})$	67	61	88	16	79	0	120	46	64	113	144	220	94	85	0	91	95	0	73	0	0
$X_4/(0.1\text{mm})$	0	51	71	31	89	164	0	50	99	11	125	89	3	163	7	0	9	4	122	115	20
$X_5/(0.1\text{mm})$	76	38	85	48	11	305	216	123	103	1	85	0	161	91	2	77	33	18	11	53	71
$X_6/(0.1\text{mm})$	77	90	150	225	64	175	92	58	306	84	1	281	5	79	30	252	3	110	32	10	40
$X_7/(0.1\text{mm})$	13	75	37	127	145	71	0	385	144	32	124	393	54	459	302	72	249	266	247	368	201
$X_8/(0.1\text{mm})$	183	263	1	183	195	286	175	189	163	0	329	129	9	354	56	67	206	391	467	364	205
$X_9/(0.1\text{mm})$	436	365	134	161	26	139	444	212	111	34	520	309	133	151	367	244	156	545	146	228	166
$X_{10}/(0.1\text{mm})$	616	571	51	91	50	504	215	3	600	284	222	336	180	156	536	1504	432	115	368	456	126
$X_{11}/(0.1\text{mm})$	175	699	275	62	223	421	137	352	211	863	15	233	760	80	197	340	401	145	320	275	785
$X_{12}/(0.1\text{mm})$	106	732	568	316	33	320	342	349	58	861	395	192	1278	126	15	115	391	1535	1313	826	398
$X_{13}/(0.1\text{mm})$	447	1646	969	253	426	230	688	477	441	343	280	608	668	351	586	1388	970	943	923	1021	100
$X_{14}/(0.1\text{mm})$	88	12	54	1217	347	351	565	75	342	371	222	170	447	561	346	297	209	749	32	67	960
$X_{15}/(0.1\text{mm})$	961	97	505	992	514	39	521	180	1468	794	378	2	304	312	62	157	786	1518	892	670	88
$X_{16}/(0.1\text{mm})$	1119	631	449	741	393	300	625	372	173	355	226	273	479	1066	790	528	1562	110	787	353	1669
$X_{17}/(0.1\text{mm})$	194	550	193	327	533	218	494	33	137	161	148	58	804	245	528	110	393	1108	203	262	0
$X_{18}/(0.1\text{mm})$	621	327	273	533	221	424	1206	443	41	121	669	591	289	812	110	790	292	188	187	238	247

## 2 Data processing and analysis

The goal of the grey correlation analysis was to explore the similarity between data sequence trends, where higher similarity indicates a higher degree of correlation in the system. When comparing the similarity between these 2 data sequences, both the numerical values and the dimensions were considered. If the data sequence was incomparable, data transformation was conducted in order to eliminate dimensions.

2.1 Feature data processing

When  $X = \{X_0, X_1, X_2, \dots, X_n\}$  was the characteristic time response data sequence of the system,  $D_1$  was the operator of the sequence, such that:

$$X D_1 = \{X_0 D_1, X_1 D_1, X_2 D_1, \dots, X_n D_1\} \text{ (Eq. 1),}$$

$$\text{and } \bar{X} = \frac{1}{n+1} \sum_{i=0}^n X_i D_1 \text{ (Eq. 2),}$$

Where  $D_1$  represents the average operator of the sequence and  $X_i D_1$  represents the average image. Then, the characteristic average image sequence data table was acquired (Table 2).

Tab.2 The characteristic average image sequence data table

	1997	1998	1999	2000	2001	2002	2003	2004	2005	2006	2007	2008	2009	2010	2011	2012	2013	2014	2015	2016	2017
$X_0 D_1$	1.98	3.75	2.45	1.58	1.49	1.33	2	1.39	0.81	0.6	0.64	0.46	0.44	0.48	0.39	0.36	0.17	0.17	0.14	0.17	0.23
$X_1 D_1$	0.13	0	0.15	0.64	1.86	0	0.71	0	0.81	2.52	0.53	3.74	1.58	0	0.46	1.04	0.18	0.94	3.1	1.02	1.6
$X_2 D_1$	0.41	3.84	0.96	1.28	0.68	0	0.02	1.26	0.96	0.56	0.08	1.18	0.83	3.63	1.41	0.06	0	0.56	2.39	0.19	0.71
$X_3 D_1$	0.97	0.88	1.27	0.23	1.14	0	1.73	0.66	0.92	1.63	2.08	3.17	1.36	1.23	0	1.31	1.37	0	1.05	0	0
$X_4 D_1$	0	0.88	1.22	0.53	1.53	2.82	0	0.86	1.7	0.19	2.15	1.53	0.05	2.8	0.12	0	0.15	0.07	2.09	1.97	0.34
$X_5 D_1$	0.99	0.5	1.11	0.63	0.14	3.98	2.82	1.61	1.35	0.01	1.11	0	2.1	1.19	0.03	1	0.43	0.24	0.14	0.69	0.93
$X_6 D_1$	0.75	0.87	1.45	2.18	0.62	1.7	0.89	0.56	2.97	0.81	0	2.73	0.05	0.74	0.29	2.44	0.03	1.07	0.31	0.1	0.39
$X_7 D_1$	0.07	0.42	0.21	0.71	0.81	0.4	0	2.15	0.8	0.18	0.69	2.2	0.3	2.56	1.69	0.4	1.39	1.49	1.38	2.06	1.12
$X_8 D_1$	0.91	1.31	0	0.91	0.97	1.42	0.87	0.94	0.81	0	1.64	0.64	0.04	1.76	0.28	0.33	1.02	1.95	2.32	1.81	1.02
$X_9 D_1$	1.82	1.53	0.56	0.67	0.11	0.58	1.86	0.89	0.46	0.14	2.18	1.29	0.56	0.63	1.54	1.02	0.65	2.28	0.61	0.95	0.69
$X_{10} D_1$	1.75	1.62	0.14	0.26	0.14	1.43	0.61	0	1.7	0.8	0.63	0.95	0.51	0.44	1.52	4.26	1.22	0.33	1.04	1.29	0.36
$X_{11} D_1$	0.53	2.11	0.83	0.19	0.67	1.27	0.41	1.06	0.64	2.6	0.05	0.7	2.29	0.24	0.59	1.02	1.21	0.44	0.96	0.83	2.36
$X_{12} D_1$	0.22	1.5	1.16	0.65	0.07	0.65	0.7	0.71	0.12	1.76	0.81	0.39	2.61	0.26	0.03	0.24	0.8	3.14	2.69	1.69	0.81
$X_{13} D_1$	0.68	2.51	1.48	0.39	0.65	0.35	1.05	0.73	0.67	0.52	4.23	0.93	1.02	0.54	0.89	2.12	1.48	1.44	1.41	1.56	0.15
$X_{14} D_1$	0.24	0.03	0.15	3.33	0.95	0.96	1.54	0.2	0.93	1.01	0.61	0.46	1.22	1.53	0.95	0.81	0.57	2.05	0.09	0.18	2.62
$X_{15} D_1$	1.8	0.18	0.94	1.85	0.96	0.07	0.97	0.34	2.74	1.48	0.71	0	0.57	0.58	0.12	0.29	1.47	2.84	1.67	1.25	0.16
$X_{16} D_1$	1.81	1.02	0.73	1.2	0.63	0.48	1	0.6	0.28	0.57	0.37	0.44	0.77	1.72	1.28	0.85	2.52	0.18	1.27	0.57	2.7

$X_{17}D_1$	0.61	1.72	0.61	1.03	1.67	0.68	1.55	0.1	0.43	0.5	0.46	0.18	2.52	0.77	1.66	0.34	1.23	3.47	0.64	0.82	0
$X_{18}D_1$	1.51	0.8	0.66	1.3	0.54	0.69	2.93	0.72	0.1	0.29	1.63	1.44	0.7	1.98	0.27	1.92	0.71	0.46	0.45	0.58	0.6

### 2.2 Grey relational degree calculation

The calculation for the grey relational degree was conducted as follows: after data transformation, the characteristic average image sequence was obtained, then the grey degree was calculated. In addition to the general relation degree, the mathematical model according to the characteristics of this system was explored, including “B,” “C,” and “T” types of grey relation degrees, as well as the degree of grey slope-correlation(Liu et al.,2013). The grey slope-correlation expresses the average change over time response sequence, system factors, and the main sequence(Wekan et al.,2011). The change tended closer,then the grey slope-correlation was larger. When investigating the influence of different precipitation periods on *D. superans* occurrence, these periods during different months exhibited a time response; this grey slope-correlation was selected for further analysis.

When  $\xi(k)$  was the correlation coefficient:

$$\xi(k) = \frac{1}{1 + \frac{|x^{(k+1)} - x^{(k)} - x^{(k+1)} - x^{(k)}|}{|x^{(k+1)} - x^{(k)}|}} \quad (i=1, 2, \dots, m; k=1, 2, \dots, n) \quad (\text{Eq. 3}).$$

When calculating the last year, “k + 1”was empty. Therefore, it was decided to stop at the “k - 1” year. This did not affect the trend of data changes. In this calculation,  $i=1, 2, \dots, 18$  and  $k=1, 2, \dots, 21$ . Then, the correlation coefficient sequence data was obtained (Table 3).

Tab.3.correlation coefficient sequence data table

	1997	1998	1999	2000	2001	2002	2003	2004	2005	2006	2007	2008	2009	2010	2011	2012	2013	2014	2015	2016
$\xi_{0k}$	0.68	0.40	0.43	0.58	0.89	0.60	0.69	0.37	0.49	0.21	0.44	0.42	0.92	0.45	0.61	0.21	0.55	0.52	0.31	0.91
$\xi_{1k}$	0.70	0.29	0.56	0.55	0.89	0.60	0.41	0.71	0.73	0.14	0.43	0.70	0.59	0.43	0.04	0.47	0.50	0.51	0.08	0.68
$\xi_{2k}$	0.64	0.55	0.20	0.54	0.89	0.60	0.46	0.50	0.56	0.87	0.58	0.43	0.84	0.81	0.48	0.46	1.00	0.45	0.85	0.79
$\xi_{3k}$	0.65	0.56	0.57	0.58	0.63	0.75	0.41	0.45	0.12	0.54	0.98	0.03	0.53	0.04	0.93	0.32	0.47	0.46	0.81	0.17
$\xi_{4k}$	0.41	0.49	0.83	0.23	0.48	0.57	0.76	0.65	0.01	0.52	0.72	0.50	0.54	0.03	0.49	0.83	0.56	0.66	0.62	1.00
$\xi_{5k}$	0.75	0.53	0.53	0.29	0.57	0.45	0.87	0.40	0.30	0.94	0.42	0.02	0.54	0.43	0.51	0.01	0.51	0.31	0.31	0.67
$\xi_{6k}$	0.73	0.67	0.44	0.84	0.52	0.75	0.41	0.51	0.24	0.60	0.48	0.14	0.56	0.78	0.24	0.35	0.94	0.88	0.87	0.48
$\xi_{7k}$	0.86	0.67	0.39	0.89	0.70	0.51	0.66	0.64	0.74	0.52	0.46	0.06	0.53	0.17	0.81	0.36	0.68	0.73	0.69	0.49
$\xi_{8k}$	0.60	0.45	0.58	0.17	0.52	0.74	0.61	0.82	0.34	0.53	0.77	0.43	0.97	0.55	0.70	0.64	0.58	0.28	0.85	0.61
$\xi_{9k}$	0.65	0.09	0.50	0.56	0.49	0.37	0.69	0.37	0.56	0.75	0.58	0.54	0.81	0.52	0.58	0.42	0.27	0.53	0.98	0.26

$\xi_{10k}$	0.78	0.49	0.26	0.56	0.63	0.29	0.49	0.94	0.48	0.02	0.43	0.59	0.10	0.55	0.67	0.44	0.36	0.57	0.75	0.72
$\xi_{11k}$	0.72	0.83	0.81	0.11	0.50	0.79	0.69	0.19	0.44	0.45	0.59	0.54	0.10	0.12	0.51	0.35	0.57	0.96	0.57	0.43
$\xi_{12k}$	0.79	0.84	0.31	0.68	0.58	0.75	1.00	0.61	0.94	0.55	0.24	0.92	0.51	0.62	0.60	0.59	0.97	0.84	0.93	0.09
$\xi_{13k}$	0.12	0.43	0.40	0.29	0.88	0.96	0.14	0.40	0.70	0.58	0.94	0.62	0.89	0.72	0.92	0.59	0.58	0.04	0.76	0.60
$\xi_{14k}$	0.10	0.43	0.49	0.54	0.07	0.63	0.41	0.39	0.67	0.47	0.72	0.50	0.94	0.22	0.60	0.34	0.67	0.67	0.66	0.12
$\xi_{15k}$	0.45	0.91	0.52	0.54	0.84	0.84	0.82	0.70	0.54	0.62	0.65	0.70	0.68	0.90	0.70	0.36	0.07	0.48	0.42	0.65
$\xi_{16k}$	0.85	0.43	0.51	0.69	0.43	0.82	0.07	0.40	0.67	0.87	0.46	0.52	0.30	0.57	0.21	0.35	0.61	0.19	0.96	0.79
$\xi_{17k}$	0.42	0.78	0.49	0.43	0.75	0.70	0.28	0.15	0.50	0.57	0.79	0.49	0.64	0.14	0.52	0.63	0.65	0.84	0.95	0.81
$\xi_{18k}$	0.68	0.40	0.43	0.58	0.89	0.60	0.69	0.37	0.49	0.21	0.44	0.42	0.92	0.45	0.61	0.21	0.55	0.52	0.31	0.91

The grey slope-correlation relation degree of  $X_0$  and  $X_i$  were donated as  $\gamma(X_0, X_i)$ , which was calculated as follows:

$$\gamma(X_0, X_i) = \frac{1}{n-1} \sum_{k=1}^{n-1} \xi_{ik} \quad (i=1, 2, \dots, m; k=1, 2, \dots, n) \quad (\text{Eq. 4}).$$

### 2.3 Simplified grey slope-correlation model

The grey slope-correlation was used to compare the correlational degree of factors over time. However, the calculating process of Eq. 3 ( $\xi^{(k)}$ ) required many calculative steps. Therefore, the computational model was simplified as follows:

$$\xi^{(k)} = \frac{1}{1 + \left| \frac{x_0(k+1)}{x_0(k)} - \frac{x_i(k+1)}{x_i(k)} \right|} \quad (i=1, 2, \dots, m, k=1, 2, \dots, n) \quad (\text{Eq. 5}),$$

where the simplified correlation coefficient,  $\xi^{(k)}$ , was affected by the denominator coefficient. When the

numerical values of  $\frac{x_0(k+1)}{x_0(k)}$  and  $\frac{x_i(k+1)}{x_i(k)}$  were similar, the data sequence curves were parallel and the variation tendencies of  $X_0$  and  $X_i$  were closer, thereby simplifying the calculation of the correlation coefficient data (Table 4).

Tab.4 The simplified correlation coefficient sequence data table

	1997	1998	1999	2000	2001	2002	2003	2004	2005	2006	2007	2008	2009	2010	2011	2012	2013	2014	2015	2016
$\xi_{1k}$	0.35	0.60	0.22	0.34	0.53	0.40	0.59	0.63	0.30	0.54	0.14	0.65	0.48	0.55	0.43	0.77	0.19	0.29	0.53	0.82
$\xi_{2k}$	0.12	0.71	0.59	0.71	0.53	0.40	0.02	0.85	0.86	0.52	0.07	0.80	0.23	0.70	0.53	0.68	0.50	0.23	0.47	0.30

$\xi_{3k}$	0.50	0.56	0.68	0.20	0.53	0.40	0.76	0.55	0.49	0.83	0.55	0.65	0.84	0.55	0.52	0.64	0.50	0.55	0.45	0.43
$\xi_{4k}$	0.35	0.58	0.83	0.34	0.51	0.40	0.59	0.42	0.61	0.09	0.99	0.52	0.02	0.57	0.52	0.68	0.65	0.03	0.79	0.46
$\xi_{5k}$	0.42	0.39	0.93	0.58	0.04	0.56	0.89	0.80	0.58	0.01	0.58	0.51	0.66	0.56	0.03	0.96	0.69	0.81	0.21	0.99
$\xi_{6k}$	0.58	0.50	0.54	0.60	0.35	0.50	0.94	0.17	0.68	0.48	0.58	0.52	0.07	0.70	0.12	0.68	0.03	0.65	0.53	0.28
$\xi_{7k}$	0.20	0.87	0.27	0.83	0.71	0.40	0.59	0.83	0.66	0.27	0.29	0.55	0.12	0.87	0.59	0.25	0.93	0.91	0.78	0.55
$\xi_{8k}$	0.69	0.60	0.61	0.89	0.64	0.53	0.72	0.78	0.57	0.48	0.75	0.53	0.02	0.60	0.80	0.28	0.52	0.73	0.70	0.56
$\xi_{9k}$	0.49	0.78	0.64	0.56	0.19	0.37	0.82	0.94	0.70	0.06	0.89	0.66	0.97	0.38	0.79	0.86	0.29	0.64	0.74	0.61
$\xi_{10k}$	0.51	0.64	0.45	0.71	0.10	0.48	0.59	0.63	0.79	0.78	0.56	0.70	0.81	0.27	0.35	0.84	0.58	0.30	0.97	0.48
$\xi_{11k}$	0.32	0.79	0.71	0.28	0.50	0.46	0.35	0.98	0.23	0.49	0.07	0.30	0.50	0.38	0.55	0.58	0.61	0.42	0.74	0.40
$\xi_{12k}$	0.17	0.89	0.92	0.54	0.11	0.70	0.76	0.71	0.07	0.62	0.81	0.15	0.50	0.59	0.12	0.26	0.25	0.97	0.63	0.53
$\xi_{13k}$	0.36	0.94	0.72	0.58	0.74	0.40	1.00	0.75	0.97	0.12	0.67	0.88	0.64	0.54	0.41	0.82	0.97	0.87	0.90	0.44
$\xi_{14k}$	0.36	0.19	0.04	0.60	0.89	0.91	0.64	0.20	0.74	0.68	0.97	0.37	0.86	0.84	0.93	0.81	0.28	0.56	0.56	0.07
$\xi_{15k}$	0.36	0.18	0.43	0.70	0.55	0.07	0.74	0.12	0.83	0.63	0.58	0.51	0.93	0.62	0.40	0.18	0.52	0.81	0.68	0.45
$\xi_{16k}$	0.43	0.94	0.50	0.71	0.88	0.63	0.91	0.90	0.44	0.71	0.68	0.56	0.47	0.94	0.79	0.29	0.52	0.14	0.57	0.23
$\xi_{17k}$	0.52	0.77	0.49	0.60	0.67	0.56	0.61	0.21	0.70	0.87	0.75	0.07	0.56	0.43	0.58	0.24	0.35	0.61	0.94	0.43
$\xi_{18k}$	0.42	0.85	0.43	0.65	0.72	0.27	0.69	0.69	0.32	0.18	0.86	0.68	0.37	0.60	0.14	0.91	0.74	0.87	0.93	0.76

Then, the simplified grey slope-correlation relation degree of  $X_0$  and  $X_i$  were marked as  $\gamma(X_0, X_i)$ , where

$$\gamma(X_0, X_i) = \frac{1}{n} \sum_{k=1}^n \xi_{ik} \quad (i=1, 2, \dots, m; k=1, 2, \dots, n) \quad \text{(Eq. 6)}$$

### 3 Results

#### 3.1 The grey slope-correlation relation degree of $X_0$ and $X_i$

From Eq.4 got the results of the grey slope-correlation relation degree were  $\gamma_{01} = 0.54$ ,  $\gamma_{02} = 0.50$ ,  $\gamma_{03} = 0.63$ ,  $\gamma_{04} = 0.50$ ,  $\gamma_{05} = 0.54$ ,  $\gamma_{06} = 0.47$ ,  $\gamma_{07} = 0.57$ ,  $\gamma_{08} = 0.58$ ,  $\gamma_{09} = 0.59$ ,  $\gamma_{010} = 0.53$ ,  $\gamma_{011} = 0.51$ ,  $\gamma_{012} = 0.51$ ,  $\gamma_{013} = 0.67$ ,  $\gamma_{014} = 0.59$ ,  $\gamma_{015} = 0.48$ ,  $\gamma_{016} = 0.62$ ,  $\gamma_{017} = 0.53$ , and  $\gamma_{018} = 0.58$ , which represent the time responses of precipitation during different months and *D. superans* occurrence. By calculating these results, it was clear that precipitation during different seasons had different degrees of correlation with *D. superans* occurrence. Specifically, precipitation during the first 10 days of July had the largest correlation ( $\gamma_{013} = 0.67$ ), and the third 10 days of March ( $\gamma_{03} = 0.63$ ) and first 10 days of August ( $\gamma_{016} = 0.62$ ) had better correlation with *D. superans* occurrence. Meanwhile, the precipitation during the third 10 days of April ( $\gamma_{06} = 0.47$ ) and the third 10 days of July ( $\gamma_{015} = 0.48$ ) correlated less with *D. superans*

occurrence.

### 3.2 The simplified grey slope-correlation relation degree of $X_0$ and $X_i$

The Eq.6 provided the following results:  $\gamma_{01} = 0.47$ ,  $\gamma_{02} = 0.49$ ,  $\gamma_{03} = 0.56$ ,  $\gamma_{04} = 0.50$ ,  $\gamma_{05} = 0.56$ ,  $\gamma_{06} = 0.48$ ,  $\gamma_{07} = 0.57$ ,  $\gamma_{08} = 0.60$ ,  $\gamma_{09} = 0.62$ ,  $\gamma_{10} = 0.58$ ,  $\gamma_{11} = 0.48$ ,  $\gamma_{12} = 0.51$ ,  $\gamma_{13} = 0.69$ ,  $\gamma_{14} = 0.58$ ,  $\gamma_{15} = 0.52$ ,  $\gamma_{16} = 0.61$ ,  $\gamma_{17} = 0.55$ , and  $\gamma_{18} = 0.60$ . The simplified grey slope-correlation of  $X_0$  and  $X_i$  revealed that the precipitation during the first 10 days of July had the best correlation ( $\gamma_{13} = 0.69$ ), which reflected the results of the classical model. In the simplified model, the top 5 groups of precipitation that had better associations with *D. superans* occurrence included the precipitation during the first 10 days of July ( $\gamma_{13} = 0.69$ ), the third 10 days of May ( $\gamma_{09} = 0.62$ ), the first 10 days of August ( $\gamma_{16} = 0.61$ ), the second 10 days of May ( $\gamma_{08} = 0.60$ ), and the third 10 days of August ( $\gamma_{18} = 0.60$ ). However, according to the classical model, the top 5 group included the first 10 days of July ( $\gamma_{13} = 0.67$ ), the third 10 days of March ( $\gamma_{03} = 0.63$ ), the first 10 days of August ( $\gamma_{16} = 0.62$ ), the second 10 days of May ( $\gamma_{08} = 0.58$ ), and the third 10 days of August ( $\gamma_{18} = 0.58$ ). The similarity between the top 5 groups of precipitation that had better associations with *D. superans* occurrence between the models was 80%.

In the simplified model, the 5 groups of precipitation that were less associated with *D. superans* occurrence included the precipitation during the first 10 days of March ( $\gamma_{01} = 0.47$ ), the third 10 days of April ( $\gamma_{06} = 0.48$ ), the second 10 days of June ( $\gamma_{11} = 0.48$ ), the second 10 days of March ( $\gamma_{02} = 0.49$ ), and the third 10 days of June ( $\gamma_{12} = 0.51$ ). In the classical model, the 5 groups that were less associated with *D. superans* occurrence included the third 10 days of April ( $\gamma_{06} = 0.47$ ), the third 10 days of July ( $\gamma_{15} = 0.48$ ), the second 10 days of March ( $\gamma_{02} = 0.50$ ), the second 10 days of June ( $\gamma_{11} = 0.51$ ), and the third 10 days of June ( $\gamma_{12} = 0.51$ ). The similarity between the 5 groups of precipitation that were the least associated with *D. superans* occurrence between the models was 80%.

### 3.3 Comparative and analysis

Considering that many complex computing models are not and cannot be widely used by forest workers or researchers, the simple grey slope-correlation model was developed to analyze the relationship between precipitation and *D. superans* occurrence. The grey slope-correlation model is able to express the average changes of many factors over a time response sequence. In this study, the grey slope-correlation model of precipitation and *D. superans* occurrence in the Xiaoxinganling Mountain Tieli forest region was constructed and the grey slope-correlation relation degree was calculated. According to the calculations and analysis of the grey slope-correlation classical model, the simplified grey slope-correlation model required fewer steps and was easier to operate. After incorporating the correlation coefficient of each month in the classical and simplified models, the correlation coefficient accumulation was obtained (Table 5).

Tab.5 The correlation coefficient accumulation table

Model	March	April	May	June	July	August
Season						
classical	$\gamma_{01} + \gamma_{02} + \gamma_{03}$	$\gamma_{04} + \gamma_{05} + \gamma_{06}$	$\gamma_{07} + \gamma_{08} + \gamma_{09}$	$\gamma_{10} + \gamma_{11} + \gamma_{12}$	$\gamma_{13} + \gamma_{14} + \gamma_{15}$	$\gamma_{16} + \gamma_{17} + \gamma_{18}$
	1.67	1.51	1.74	1.55	1.74	1.73

	$\gamma_{01} + \gamma_{02} + \gamma_{03}$	$\gamma_{04} + \gamma_{05} + \gamma_{06}$	$\gamma_{07} + \gamma_{08} + \gamma_{09}$	$\gamma_{10} + \gamma_{11} + \gamma_{12}$	$\gamma_{13} + \gamma_{14} + \gamma_{15}$	$\gamma_{16} + \gamma_{17} + \gamma_{18}$
simplified	1.52	1.54	1.79	1.57	1.79	1.76

The correlation coefficient accumulation during May and July had good measure in both models. This indicates that the precipitation during May and July were the greatest contributing precipitation factors on *D. superans* occurrence compared to others period. Similar results were found by previous studies that used a different analysis method (Ma, 2017; Yu *et al.*, 2016). Although both models exhibited different correlation coefficient accumulations, both models indicated that the precipitation period that contributed the least was during the spring. Moreover, the results of the models were similar, where the precipitation during May and July had the greatest associations with *D. superans* occurrence, but the simplified model required fewer calculative steps.

## 4 Discussion

### 4.1 Critical precipitation period for *D. superans*

According to the results, precipitation during May ( $\gamma_{07} + \gamma_{08} + \gamma_{09} = 1.74$ ,  $\gamma_{07} + \gamma_{08} + \gamma_{09} = 1.79$ ) and July ( $\gamma_{13} + \gamma_{14} + \gamma_{15} = 1.74$ ,  $\gamma_{13} + \gamma_{14} + \gamma_{15} = 1.79$ ) had the greatest associations with *D. superans* occurrence. In previous studies, the larval stage and breeding season were found to be the critical periods for *D. superans* (Yang *et al.*, 2014; Yu *et al.*, 2016). The life cycle of *D. superans* can be divided into the larval, larger larval, pupa, eclosion, adult, and spawning stages. *D. superans* produces 1 generation a year and overwinters as larvae in the Tieli forest region. The larval stage lasts for 3 seasons in Northeast China. Larvae hatch in autumn, stay in the litter layer during the winter, and finally climb up the trees during the spring of the next year. Precipitation has a great effect on *D. superans* occurrence. Aside from precipitation, temperature is also a critical factor that affects the larvae's ability to climb trees, while warm and dry climatic conditions benefit larval growth (Liu, 1994; Tiit *et al.* 2010). Precipitation during the third 10 days of March ( $\gamma_{03} = 0.63$ ,  $\gamma_{03} = 0.56$ ) was found to be the most important time period affecting *D. superans* occurrence compared to the other time periods in March. Because more precipitation tends to increase humidity, the additional humidity disturbs the water balance in insects, leading to epidemics of pathogenic microorganisms. Precipitation during the late spring promotes tree growth and provides food for larvae. When larvae experience high humidity for long periods of time, the body water loss balance can cause developmental delays or abnormalities (Chen *et al.* 2011; Abdul *et al.* 2014).

In the *D. superans* breeding season (July, August), precipitation during the first 10 days of July ( $\gamma_{13} = 0.67$ ,  $\gamma_{13} = 0.69$ ) was found to be the most important factor affecting *D. superans* occurrence. This finding was similar to the results of a previous study on climate change and the occurrence of crop insects, where occurrence and precipitation exhibited a positive correlation. When the average annual precipitation and heavy rainfall increased by 1 mm, pest occurrence rates increased by 0.004 and 0.008 and pest occurrence increased by  $59.5 \times 10^4$  and  $11.89 \times 10^4$  hm<sup>2</sup>, respectively. Thus, precipitation clearly facilitated migratory pest decent and increased the base number of insects (Zhang *et al.*, 2012). Moreover, precipitation influences pest food sources (i.e., trees and others plant), their natural enemies (e.g., *trichogramma*), and other biotic factors (Vladimir *et al.*, 2016)

### 4.2 Application of greysystemtheory

The application of greysystemtheory requires less data input than the multiple linear regression analysis method, and the calculations are simple and easy to operate (Abdul et al., 2019; Zhang et al., 2019). Specifically, the selected meteorological index was easy to calculate and the system had no force requirement due to its simple capacity and regularity. Moreover, grey slope-correlation can reveal the correlational degree of factors over time (Wekanet al.2011). The simplified correlation coefficient was affected by the denominator coefficient, while the simplified model was easy to calculate, required fewer steps, and had 80% similarity with the classical model. The findings of this study can provide a theoretical reference for pest forecasting and early warning. This simple method was used to uncover the most critical periods of precipitation affecting pestoccurrence, which was found to be the first 10 days of July. Thus, the grey system theory can be widelyused by forest workers and researchers. Monitoring precipitation during the first 10 days in July should be a focus, and when the precipitation of the first 10 days in July increases while other factors are consistent, precautions should be implemented the next spring.

Different precipitation periods from March to August were measured by the weather service department. While *D. superans* was prone to sprawling, occurrence was the main time response sequence data that was difficult to calculate. In this study, occurrence data was obtained from actual measurements and empirical prediction, but its scientific foundation and precision needs to be improved. The period of precipitation with the greatest effect on pest occurrence was the first 10 days of July, which corresponds with the breeding season of *D. superans*. However, the life stages of this pest overlap in time and determiningwhich pest stage (i.e., feathering, spawning, or hatchingperiods) was affected by which precipitation period was difficult to discern. Therefore, refinement of this scientific model requires further investigation.

## 5 Conclusion

The grey slope-correlation model can uncover the correlation degree of factors over time. The simplified model required steps and had 80% similarity to the classical model. Both models revealed that precipitation during the first 10 days of July had the greatest correlation ( $\gamma_{13} = 0.67$ ,  $\gamma'_{13} = 0.69$ ) with *D. superans* occurrence, while the first 10 days of August ( $\gamma_{16} = 0.62$ ,  $\gamma'_{16} = 0.61$ ), the second 10 days of May ( $\gamma_{08} = 0.58$ ,  $\gamma'_{08} = 0.60$ ), and the third 10 days of August ( $\gamma_{18}=0.58$ ,  $\gamma'_{18}=0.60$ ) also had large correlations with *D. superans* occurrence. However, the least-correlated time periods of precipitation affecting*D. superans* occurrence were quite different between the two models. The classical model showed that the third 10 days of April ( $\gamma_{06} = 0.47$ ) were the least correlated, while the simplified model showed that the first 10 days of March ( $\gamma'_{01} = 0.47$ ) was the least correlated with *D. superans* occurrence. When adding the correlation coefficients of each month in the classical and simplified models, the correlation coefficient accumulation in May and July had good measures in both models. Thus, precipitation during May and July was clearly the most important precipitation factor affecting *D. superans*' occurrence, while precipitation during the spring was the least important precipitation factor.

## References

- [1]Abdul HAS,MuhammadI,RanaMA,HamzaQ,Muhammad N(2019) Evaluation of key factors influencing process quality during construction projects in Pakistan. Grey Systems: Theory and Application 9(3):321-335
- [2]Abdul K,MuhammadJ,MubasshirS,Muhammad S(2014)Environmental effects on insects and their population dynamics.J of Entomology and Zoology Studies 2(2):1-7
- [3]Bakke A (1992) Monitoring bark beetle populations: effects of temperature.Applied Entomology 114: 208-211



- [4]Chon TS,ParkYS,KimJM,LeeBY,ChungYJ,Kim YS(2000)Use of an artificial neural network to predict population dynamics of the forest-pest Pine Needle gall midge (Diptera: Cecidomiida). *Environmental Entomology* 29(6):1208-1215
- [5]Chen SH, Zhang XL (2011) Meteorological conditions and area forecast for occurrence of *Dendrolimus superans* in inner Mongolia.*J of Northeast Forestry University* 39(11):135-136.Chinese
- [6]Chen YT, Vasseur L, You MS (2017) Potential distribution of the invasive loblolly pine mealybug, *Oracella acuta*(Hemiptera:Pseudococcidae),in Asia under future climate change scenarios. *Climatic Change* 141(4):719-732.Chinese
- [7]Cao MX(2007)Research on grey incidence analysis model and its application.Nanjing University of Aeronautics and Astronautics p7-12.Chinese
- [8]Cao MX,DangYG,ZhangR,Lu JF(2007)Improvement of grey relational degree calculation method.*Statistics& Decision* 2007(07):29-30.Chinese
- [9]Dang YQ, Wang XY, Yang ZQ (2018) Advances in biological control of forest insect pests by using natural enemies in China. *Journal of Environmental Insect* 40(2):242-255.Chinese
- [10]Feng HM, Yan W, Li XF (2013) Non-linear prediction of insects based on Choquet integral. *Hubei Agricultural Science* 52(22):5485-5487.Chinese
- [11]Kang US(2005)Study on the classification of forest pest occurrence region(FPOP) in DPR of Korea.In:Proceedings of International Symposium on Ecological Conservation and Sustainable Development of Forest Resources in Northeast Asia(<http://xueshu.baidu.com/usercenter/paper/show?paperid=89e8477aab43a9b720ccd437ee49d07&site/02/10.html>)
- [12]Kumar S,NevenLG,ZhuHY,Zhang RZ (2015) Assessing the Global Risk of Establishment of *Cydia pomonella* (Lepidoptera: Tortricidae) using CLIMEX and MaxEnt Niche Models.*J of Economic Entomology* 40(5): 127-138.
- [13]Liu KY (1994) Causes of outbreak of the larch caterpillar (*Dendrolimus superans* Butler) in Daxingan Mountain and its control strategy.*J of Northeast Forestry University* 5(1):31-40.
- [14]Liu SF,Xie NM.2013. Grey systems theory and the application.SciencePress,Beijing,p 48-59.Chinese
- [15]Li ZR,LiQG,FanDW,ZhangBH,ZhangFJ,QuZ,Wang J (2019) Grey correlation analysis of meteorological variation and pest occurrence.*Forest Engineering* 35(4):51-57.Chinese
- [16]Ma XB (2017) Temperature and humidity effects on *Dendrolimus superans* butler grow and develop.Harbin,NortheastForestry University p 25-31.Chinese
- [17]Myong SJ,DohongK,Se KY(2012) *Lepidopterous* insect fauna of Ui-do Island in Korea,*J of Korean Nature* 5(3):221-226.
- [18]Marchisio C, CescattiA,Battisti A(1994) Climate soils and *Cephalica arvensis* outbreaks on Piceaabies in the Italian Alps.*Forest Ecology and Management* 68(2-3): 375-384.
- [19]Natalia IK,Yuri N. Baranchikov,Stefan V(2009) Performance of the potentially invasive Siberian moth *Dendrolimus superans*sibiricus on coniferous species in Europe.*Agricultural and Forest Entomology* 11(3):247-254.
- [20]NieXB,ChengXC,ChuFG,ZhouMJ,SunSP,Xu ZC (2017) The preliminary study on biology characteristics and population influencing factors of *Lymantria mathura*Moore.*Forest Pest and Disease* 36(3):22-25.Chinese
- [21]RatheeS,Kashyap A (2018)Adaptive-miner:an efficient distributed association rule mining algorithm on spark.*J of Big Date* 5(1):1-17.
- [22]Tiit T, Toomas E, Triinu R, Anu S, Toomas T (2010) Counterintuitive size patterns in bivoltine moths:late-season larvae grow larger despite lower food quality. *Oecologia* 162(1):117-125
- [23]Tang HY,Niu BL (2010)Influence of meteorological factors on reproduction of *Dendrolimus superans* and forecast of spawning quantity. *Journal of Northeast Forestry University* 38(1):84-87.Chinese
- [24]Tomin FN,OsinaOV,KuzubovAA,OvchinnikovSG,Volkova TM, Ovchinn TM (2011) Stability of forest *lepidopteran pheromones* against environmental factors.*Biophysics* 56(4):714-722.
- [25]Vladimir G,SvetlanaG,Jose' M.2016.Common infectious diseases of insects in culture diagnostic and prophylactic methods, Springer,New York,P 53-57.
- [26]Wermelinger B,M Seifert (1998) Analysis of temperature dependent development of the spruce bark beetle *Ips typographus*.*Applied Entomology* 122:185-191.

- [27]WekanK,IzzettinT,Serpil E (2011) Grey system approach for economic order quantity models under uncertainty.The J of Grey System 23(1):71-82.
- [28]Xu YM.2015. The practical diagram of forest pest control techniques. Chemical Industry Press, Beijing p 38-40.Chinese
- [29]Yu Y,FangL,FangGF,WangFX,Yang J (2016) Influences of meteorological factors on *larch caterpillar* population. Chinese J of Applied Ecology 27(9):2839-2847.Chinese
- [30]Yang SX , Zhao HY , Bao XH (2014) A study on the Forecast model of *Dendrolimus superans* Burler occurrence based on Artificial Neural Network.Chinese Agricultural Science Bulletin 30(28):72-75.Chinese
- [31]Zhang L,HuoZG,WangL,Jiang YY (2012) Effects of climate change on the occurrence of crop insect pests in China.Chinese Journal of Ecology 31( 6) : 1499-1507.Chinese
- [32]Zhang WY,JingTZ,Yan SC (2017) Studies on prediction models of *Dendrolimus superans* occurrence area based on machine learning.J of Beijing Forestry University 39(1):85-93. Chinese
- [33]Zhang YL,Peng F, Mu JL (2019) The Application of Grey System Theory on the Corrosion Behavior of Steel in Seawater.J of The Institution of Engineers (India): Series C, 100 (4):693-699.